17,000 YEARS OF CLIMATE CHANGE:

THE PHYTOLITH RECORD FROM HALL'S CAVE, TEXAS

By

JASON PAUL JOINES

Bachelor of Science in Geography

Oklahoma State University

Stillwater, Oklahoma

2005

Submitted to the Faculty of the
Graduate College of the
Oklahoma State University
in partial fulfillment of
the requirements for
the Degree of
MASTER OF SCIENCE
December, 2011

17,000 YEARS OF CLIMATE CHANGE:

THE PHYTOLITH RECORD FROM HALL'S CAVE, TEXAS

Thesis Approved:

Dr. Carlos E Cordova

Thesis Adviser

Dr. Michael W. Palmer

Dr. Alexander R. Simms

Dr. Sheryl A. Tucker

Dean of the Graduate College

TABLE OF CONTENTS

INTRODUCTION **1**
Acknowledgements 1
Author Contributions 2
CHAPTER 1. 17,000 YEARS OF CLIMATE CHANGE: THE PHYTOLITH RECORD FROM HALL'S CAVE, TEXAS **3**
Abstract 3
Introduction 4
Study Site 5
Materials and Methods 5
Sampling and processing 5
Quantitative Analysis 6
Zone determination 6
Transfer functions and statistical significance 7
Phytolith indices 7
Results 8
Zone 4 (17,550 – 16,040 BP, 250 - 215 cm) 8
Zone 3 (15,510 - 8170 BP, 205 - 105 cm) 9
Zone 2 (7750 - 2900 BP, 100 - 40 cm) 10
Zone 1 (2560 - 730 BP, 35 - 0 cm) 10
Discussion 11
Reconstructed Climate 11
Reconstructed Vegetation 13
Issues and Limitations 14
Conclusions 16
References 16
Appendix. Supplemental electronic data 35

LIST OF TABLES

Table 1: Sample depths, ages, and associated lithology. Ages are in calibrated ^{14}C years after Ellwood and Gose (2006). Lithology is from Toomey (1993) and Ellwood and Gose (2006).....20

Table 2: Phytolith morphotypes as counted, their mapping onto the classification of Lu et al. (2006), use and classification in the calculation of I_W, and use and classification in calculation of I_C.....23

LIST OF FIGURES

Figure 1: Location of Hall's Cave and the Edwards Plateau.....26

Figure 2: Phytolith morphotypes counted with at least five percent abundance in at least one sample. Morphotype abbreviations are: epipoly = Epidermal polygonal, scallfacet = Scalloped faceted, roundblock = Round blocky, otherlong = Other long cells, square = Square, othershort = Other short cells, fan = Fan, shortsaddle = Short saddles, rectangle = Rectangular, celtis = Celtis type, broadlong = Board elongate, flatower = Flat towers, longpoint = Long point.....27

Figure 3: Phytolith morphotypes used in transfer functions with non-zero percentage in at least one sample. Morphotype abbreviations are: Gymno = Gymnosperm types, Broad = Broad-leaf-type, Dumbb = Panicoid (Dumbbell and cross), LongS = Long saddle, ShortS = Short saddle, WavyT = Wavy-trapezoid, WavyN = Wavy-narrow-trapezoid, Ronde = Rondel, FanBa = Fan-bamb, Fan = Fan, Square = Square, Recta = Rectangle, Board = Board-elongate, Sinua = Sinuate-elongate, Smoot = Smooth-elongate, LongP = Long-point, ShortP = Short point, Gobbet = Gobbett (nubby-irregular shape).....28

Figure 4: MAT reconstructed mean annual precipitation. Vertical dotted lines represent zone boundaries. Horizontal dashed line shows modern value of mean annual precipitation. Error bars indicate $RMSEP_{loo}$.....29

Figure 5: MAT reconstructed mean annual temperature. Vertical dotted lines represent zone boundaries. Horizontal dashed line shows modern value of mean annual temperature. Error bars indicate $RMSEP_{loo}$.....30

Figure 6: Dissimilarity values (squared chord distance) for mean annual precipitation (green, k = 6) and mean annual temperature (red, k = 14). Horizontal dashed line represents optimal dissimilarity value determined by ROC analysis. Vertical dotted lines represent zone boundaries. Minimum possible dissimilarity is 0 and maximum is 2.....31

Figure 7: Phytoliths from grasses and woodies used in the calculation of I_W as percentage of total phytoliths along with I_W.....32

Figure 8: Phytoliths attributed to grass sub-families dominated by the C_3 or C_4 or photosynthetic pathway and used in the calculation of I_C along with I_C. I_C shown only for samples where total phytoliths used in calculation totaled at least 30.....33

INTRODUCTION

Acknowledgements

I would like to thank my advisor, Carlos Cordova, and my committee members, Mike Palmer and Alex Simms, for their guidance and support throughout this thesis project and degree program. In particular, I would like to thank Carlos for inspiring me to launch a second career and start down this path. Carlos has always been approachable and generous with his time, and I appreciate that he was willing to take me under his wing even before I became an "official" graduate student. Likewise, I would like to thank Mike Palmer and his former student Dan McGlinn for including me in their lab activities, even before I was an "official" graduate student. Mike and Dan allowed me to work with them on two different forest survey projects and took me to my first ESA meeting. They have inspired me pursue the next step in my academic career.

I would also like to thank Ernest Lundelius whose idea started this thesis project. Ernest was overly generous with his time, facilities, equipment, and assistance, and was generally great to be around during the field work portion of this project. I am also thankful to Billie Hall for allowing us to user her ranch as our field site. We literally couldn't have completed this project without her support. Byron Sudbury was overly generous with his time while training me to use a particularly tricky slide mounting medium. He was also too generous in donating lab supplies that proved to be invaluable to me, and I appreciate the support and encouragement he kept coming throughout this project.

I would also like to express my thanks to practically every graduate student in Botany, NREM, and Zoology who've passed through Stillwater over the last several years, along with a few scattered out in other areas as well. Their comradery and friendship has made this entire endeavor truly enjoyable. Among them are Scott Fine and Ramin Zamanian who all too often served as involuntary sounding boards for ideas I had and issues I encountered along the way. I'm especially thankful of Jessica O'Connell who heard about my project more often than any other person. Not only did she provide great feedback and advice, but I couldn't have completed this project without her daily support, encouragement, and companionship.

Author Contributions

The only chapter of this thesis, "17,000 Years of Climate Change: The Phytolith Record from Hall's Cave, Texas", is a manuscript I coauthored with my advisor Carlos Cordova along with Ernest Lundelius. Ernest had the idea that initiated this project. He facilitated access to the field site, allowed us the use of his lab, provided field equipment, and worked with Carlos and I to collect samples. He has also provided valuable ideas and insight throughout this project. I extracted the phytoliths from the sediment samples and mounted them on microscope slides. Carlos performed the classification and counting of phytoliths. I performed the analysis and writing with much feedback and guidance from Carlos. We will submit this manuscript to an appropriate scientific journal.

CHAPTER 1. 17,000 YEARS OF CLIMATE CHANGE: THE PHYTOLITH RECORD FROM HALL'S CAVE, TEXAS

Abstract

We used modern analog technique to develop phytolith-based transfer functions. We applied these transfer functions to phytolith assemblages in sediments from Hall's Cave, Texas to reconstruct mean annual precipitation and temperature for the central Edwards Plateau from 17,550 BP to 730 BP and tested these reconstructions for statistical significance. We also interpreted the phytolith assemblage and applied phytolith indices of woody cover and of C_3 versus C_4 grasses to reconstruct Edwards Plateau vegetation over the same period.

Reconstructed mean annual precipitation (RMAP) was less than 450 mm during the last glacial period with the exception of a spike to over 1150 mm at 17,160 BP. As glacial conditions ended RMAP progressively increased with oscillations between modern (800 mm) and higher values until reaching a high of over 1200 mm at 9860 BP. Then RMAP gradually decreased to less than 825 mm at 6890 BP followed by a gradual increase to over 1325 mm at 2560 BP. RMAP then dropped sharply to less than 625 mm at 1640 BP followed by an increase to above modern values by 730 BP. Reconstructed mean annual temperature (RMAT) followed a similar trend. RMAT was much cooler than present with a minimum of less than 10 °C during the last glacial period. RMAT also spiked at 17,160 BP approaching 15 °C before declining again. After glacial conditions ended RMAT generally increased reaching 17 °C by 3620 BP. After 2560 BP RMAT declined sharply to near 12.5 °C at 1640 BP before increasing again reaching 14 °C by 730 BP. RMAP proved to be statistically significant. We also have confidence in the trend exhibited by RMAT but temperatures may be underestimated.

Vegetation on the Edwards Plateau near the end of the last glacial period was open woodland or savanna with mixed C_3 and C_4 grasses changing to closed woodland by 16,740 BP and transitioning to forest by 14,940 BP with grasses nearly absent. Forest with little or no grass was the most common vegetation for the next 12,000 years. Open woodland or savanna with mixed C_3 and C_4 grasses re-appeared at 2560 BP transitioning to a mixed C_3 and C_4 grassland by 2230 BP and to C_4 grassland by 730 BP.

Introduction

Several researchers have used sediments from Hall's Cave to reconstruct paleoenvironmental conditions on the Edwards Plateau. Toomey et al. (1992) analyzed stable carbon isotope ratios from the bones of extinct grazers found in the cave to determine the ratios of C_3 and C_4 grasses on the plateau from 16,040 to 15,720 BP. Toomey et al. (Toomey, 1993; Toomey et al., 1993) reconstructed climatic conditions and vegetation from 20,000 to 1000 BP using the remains of fauna and analysis of their habitat requirements. Cooke et al. (2003) used strontium ratios from sediments, seed coatings, and tooth enamel found in the cave to reconstruct soil erosion for the past 21,000 years. Ellwood and Gose (2006) measured magnetic susceptibility of Hall's Cave sediments for reconstruction of climatic changes from the Last Glacial Maximum (LGM) until 500 BP

Previous studies have used modern phytolith assemblages to develop models for quantitative reconstruction of environmental variables (Fredlund and Tieszen, 1997; Prebble et al., 2002; Lu et al., 2006). Fredlund and Tieszen (1997) reconstructed mean July temperatures in the Great Plains of North America since the Pleistocene-Holocene transition. Prebble and Shulmeister (2002) applied their transfer functions to the reconstruction of soil pH and conductivity, mean annual precipitation, and mean autumn temperature in New Zealand since the Last Glacial Maximum as well as for the Last Interglacial. Lu et al. (2007) reconstructed mean annual precipitation and mean annual temperature for the Loess Plateau in China over the past 136 ka.

Lu et al. (2006) created a modern data set from phytolith assemblages collected in seven different vegetation types at 243 sites covering gradients in mean annual precipitation of 1915 mm and mean annual temperature of over 27 °C. The variety of vegetation, large sample size, and wide climatic gradients make this an ideal data set for development of transfer functions for application to paleoenvironmental reconstructions.

Climatic reconstructions at Hall's Cave based on faunal analyses were only able to pick up general trends (Toomey, 1993; Ellwood and Gose, 2006) and vegetation reconstructions based on faunal analyses were problematic (Toomey, 1993). Similarly, Ellwood and Gose (2006) were only able to pick out general climatic trends and exceptional climatic events using magnetic susceptibility of Hall's Cave sediments. None of the Hall's Cave reconstructions were based directly on the remains of plants. Here we attempt higher resolution reconstructions of climate and vegetation based on phytolith assemblages from Hall's Cave using climatic transfer functions developed from the data set published by Lu et al. (Lu et al., 2006).

Study Site

Hall's Cave is located in the central Edwards Plateau (Fig. 1) near the town of Mountain Home in Kerr County, Texas. Data for the years 1931 through 2010 (National Climatic Data Center, 2011) from the nearest meteorological stations in Kerrville show mean annual temperature of 18 °C and mean annual precipitation of 800 mm. Precipitation has a bimodal distribution with the first peak occurring in the months of May and June followed by the second peak in September and October. Mean annual precipitation follows a strong east to west gradient across the plateau ranging from as much 863 mm along the eastern edge to as little as 407 mm along the western edge. There is little variation in mean annual temperature across the plateau. Vegetation ranges from typical eastern deciduous forest in sheltered canyons on the eastern edge of the plateau to shrubland dominated by *Prosopis glandulosa* in the west following the precipitation gradient across the plateau. Less disturbed vegetation in the area of Hall's Cave is typically savanna or open woodland characterized by *Quercus fusiformis*, *Q. buckleyi*, and *Juniperus ashei*, (Griffith et al., 2007) with both tall and short grasses including *Panicum virgatum*, S*orghastrum nutans*, *Schizachyrium scoparium*, and *Bouteloua curtipendula* (Riskind and Diamond, 1988). Riparian areas contain more forest including species of *Carya*, *Fraxinus*, *Juglans*, *Platanus*, *Populus*, *Salix* and *Ulmus* (Griffith et al., 2007).

The cave consists of one large room accessible by a sinkhole opening upslope. This opening has facilitated sediment washing into the cave from a 3 ha area, accumulating to a depth of over 3 m in places (Toomey, 1993). Work in the cave by several researchers has resulted in an excavation pit with a well dated stratigraphy (Toomey, 1993; Toomey et al., 1993; Cooke et al., 2003; Ellwood and Gose, 2006). Hall's Cave is the only known Edwards Plateau cave with continuous stratigraphy from the Pleistocene to the present (Toomey, 1993; Toomey et al., 1993).

Materials and Methods

Sampling and processing

After removing recent fill from the existing pit, we collected sediment samples at 5 cm intervals down to a depth of 250 cm below the zero datum established by Toomey (1993) except where collection was made impossible by the rocky nature of the sediment (200, 210, 220, and 225 cm). Ages of these samples range from 730 to 17,550 BP (^{14}C years, calibrated) based on the chronological model of Ellwood and Gose (2006). Sample depths, ages, and associated lithology are shown in Table 1.

Our procedure for phytolith extraction from sediments is based on methods reviewed by Lentfer and Boyd (1998) and Zhao and Pearsall (1998) and consists of the following steps:

(1) Grind sample gently with pestle and mortar.
(2) Sieve sediment sample through 125 µm mesh to remove large particles. Repeat (1) and (2) until approximately 1 g of sieved sample has been obtained.
(3) Transfer sample to 50 mL centrifuge tube. Pipette 35 % HCl into tubes until reaction has stopped to remove carbonates. Stir sample. Centrifuge at 2700 RPM for 3 minutes and decant. Fill tubes with deionized water, centrifuge and decant. Continue until supernatant has a neutral pH.
(4) Pipette 10 % KOH into tubes in volume approximately double that of the sample to remove organics. Stir sample. Centrifuge at 2700 RPM for 3 minutes and decant. Fill tubes with deionized water, centrifuge and decant. Continue until supernatant has a neutral pH.
(5) Fill beaker to 10 cm depth with 0.5 % $NaPO_3$ to deflocculate clays. Add sample and stir. Allow to settle for 2 hours, then decant. Continue until supernatant is clear to remove clays.
(6) Transfer sample to 15 mL centrifuge tube. Centrifuge at 2700 RPM for 3 minutes and decant. Add low-viscosity sodium polytungstate with specific gravity 2.3 in volume approximately triple that of the sample. Stir sample. Centrifuge at 1100 RPM for 10 minutes. Pipette supernatant to second 15 mL centrifuge tube to isolate biogenic silica. Fill second 15 mL centrifuge with deionized water, centrifuge at 2700 RPM for 3 minutes then decant. Repeat centrifuge with deionized water and decant 3 times to remove all sodium polytungstate from sample.
(7) Pipette samples to aluminum weighing dish and oven dry.

After extraction we mounted phytoliths on slides in Canada balsam for counting and classification. We divided phytoliths into 49 types (Table 2) after the classification used by Cordova et al. (2011) with additions, and mapped these types onto the 21 types used by Lu et al. (2006) (Table 2) for the purpose of transfer function development. We counted a minimum of 300 phytoliths per sample (Appendix).

Quantitative Analysis

Zone determination

We performed a stratigraphically constrained hierarchical cluster analysis using the CONISS algorithm (Grimm, 1987) with only known morphotypes with an abundance of at least five percent of the total phytoliths in any sample (Birks and Berglund, 1979) to delineate zone boundaries. We applied the broken stick method described by Bennett (1996) to determine the number of significant zones.

For both zone delineation and determination of the number of significant zones we used the

package rioja 1.0-0 (Juggins, 2011) with R 2.13.2 (Team, 2011).

Transfer functions and statistical significance

Lu et al. (2006) developed transfer functions using weighted averaging partial least squares (WA-PLS) (ter Braak and Juggins, 1993). We used modern analog technique (MAT) (Overpeck et al., 1985) instead. According to Telford and Birks (2011), when the number of effective species in an assemblage is low, reconstructions based on weighted averaging methods are unlikely to be statistically significant and MAT-based reconstructions should be tested. Our assemblage had a low number of effective taxonomic units, 3.3 as estimated by Hill's N2 diversity index (Hill, 1973). We applied MAT with the squared chord dissimilarity metric to the training data set published by Lu et al. (2006) to create transfer functions for reconstructing mean annual precipitation (RMAP) and mean annual temperature (RMAT). We selected the best model by choosing the number of components that minimized RMSEP as determined by leave-one-out cross-validation.

Using the method developed by Telford and Birks (2011), we then tested the statistical significance of both our MAT-based reconstructions and reconstructions using the WA-PLS models of Lu et al. (2006). For each significance test we generated 10000 transfer functions trained on random data.

As an additional measure of confidence in the model predictions, we used the Receiver Operating Characteristic (ROC) analysis described by Wahl (2004) to determine analog versus non-analog cutoff values for the squared chord distance metric.

We used R 2.13.2 (Team, 2011) with the package rioja 1.0-0 (Juggins, 2011) to generate transfer functions, package palaeoSig 1.0 (Telford, 2011) for significance tests, and package analogue (Simpson and Oksanen, 2011) for ROC analysis.

Phytolith indices

As an index of woody cover, I_W, we examined the woody phytolith morphotype percentage of the sum of woody and grass morphotypes. This is essentially the phytolith woodland-grassland index (PWGI) defined by Cordova et al. (2011) converted to percentages. Table 1 shows the use of morphotypes in this index. In terms of percentages, Cordova et al. (2011) observed that across the Great Plains PWGI values below 33 % are typical of open grassland, values between 33 and 67 % are indicative of savanna or open woodland, values between 67 and 80 % are representative of closed woodland, and values over 80 % indicate closed canopy forest.

We also analyzed the C_3 grass short cell morphotype percentage of the sum of C_3 and C_4 grass

short cell morphotypes, I_C, as proposed by Twiss (1987). Barboni et al. (1999) used data from the Great Plains published by Fredlund and Tieszen (1994) to calculate I_C. They showed that values over 70 % where typical of cool northern C_3 grasslands while values less than 30 % represented warmer southern C_4 grasslands.

Results

Figure 2 summarizes phytolith morphotype abundances as counted while Figure 3 shows abundances for the classification used in reconstructions. Cluster analysis resulted in four significant zones which are shown in Figures 2 through 7.

The best MAT model for mean annual precipitation was the 6-analog weighted mean transfer function with $RMSEP_{loo}$ = 150.0 mm, R^2_{loo} = 0.8899 and significance of p = 0.0049. For mean annual temperature the best model was the 14-analog weighted mean transfer function with $RMSEP_{loo}$ = 2.294 °C, R^2_{loo} = 0.8579, and significance of p = 0.1027.

Figures 4 and 5 show results of MAT-based RMAP and RMAT respectively. Reconstructions for mean annual precipitation and mean annual temperature based on the WA-PLS models of Lu et al. (2006) had significance of p = 0.1547 and p = 0.4606 respectively. We only refer to the MAT-based reconstructions in the following results and discussion.

ROC analysis resulted in optimal dissimilarity cutoff values of 0.1580 for mean annual precipitation and 0.1560 for mean annual temperature. Figure 6 summarizes dissimilarity values.

Figures 7 and 8 summarize the changes in abundance of woody and grass phytolith morphotypes as well as the changes in abundances of morphotypes associated with C_3 versus C_4 photosynthesis.

Zone 4 (17,550 – 16,040 BP, 250 - 215 cm)

The phytolith assemblage in zone 4 was dominated by unclassified morphotypes which accounted for over 55 % of total phytoliths and made up the largest category in every sample. Round blocky, epidermal polygonal, and scalloped faceted were the most abundant classified morphotypes.

RMAP was 689 ± 300 mm for zone 4 with minimum of 434 mm at 17,550 BP. RMAP rose to a maximum of 1162 mm at 17,160 BP, followed by a decrease to near the minimum level at 16,960 BP. RMAP then rose to modern levels at 16,740 BP and began a gradual decline. RMAT was 12.3 ± 2.1 °C with minimum of 9.8 °C at 17,550 BP rising to a maximum of 14.6 °C at 17,160 BP. RMAT then decreased followed by a rising trend continuing into zone 3.

RMAP had mean dissimilarity of 0.48 with mean sample dissimilarity minimum of 0.39 at 17,550

BP and mean dissimilarity maximum of 0.59 at 16,040 BP. RMAT mean dissimilarity was 0.72 with mean sample dissimilarity minimum of 0.43 at 17,550 BP and mean dissimilarity maximum at 16,040 BP of 0.66. There were no dissimilarities less than 0.1580.

I_W was 57 ± 20 % with minimum at 17360 BP of 35 %. Maximum values of 78 and 80 % occurred at 16,740 and 16,040 BP respectively. I_C was 63 ± 14 % with minimum of 47 % at 17,550 BP and maximum of 88 % at 16,740 BP

Zone 3 (15,510 - 8170 BP, 205 - 105 cm)

Unclassified morphotypes dominated the phytolith assemblage in zone 3 comprising 49 % of total phytoliths. Unclassified morphotypes made up the largest category for all but two samples. The epidermal polygonal morphotype was most abundant in samples 14,940 BP and 10,280 BP with 53 and 39 % respectively. The most abundant classified morphotypes were epidermal polygonal, scalloped faceted, and round blocky.

RMAP was 944 ± 142 mm for zone 3. The decline that began in zone 4 continued until reaching a minimum of 574 mm at 14,940 BP. This decline was followed by a steep rise to near maximum values with 1132 mm at 14,000 BP. RMAP then dropped sharply to 967 mm at 13,670 BP followed by another increase to near maximum values at 13,330 BP with 1165 mm. RMAP then began a general decline reaching modern values at 11,870 BP. RMAP reached near maximum values again with 1180 mm at 11,090 BP, then decreased to modern values by 10,280 BP followed by an increase to a maximum of 1220 mm at 9860 BP. RMAP then began a general decreasing trend continuing throughout the zone. RMAT was 14.9 ± 1.5 °C continuing the increasing trend began in zone 4 before decreasing to a minimum of 11.9 °C at 14,640 BP. After reaching minimum, RMAT generally increased throughout the zone with maximum of 16.9 °C occurring at 11,090 BP

RMAP had mean dissimilarity of 0.61 with mean sample dissimilarity minimum of 0.47 at 15,510 BP and mean sample dissimilarity maximum of 0.66 at 14,000 BP. RMAT mean dissimilarity was 0.70 with mean sample dissimilarity of 0.52 at 15,510 BP and mean sample dissimilarity maximum at 14,000 BP of 0.78. There were no dissimilarities less than 0.1580.

I_W was 87 ± 10 % with minimum of 57 % at 15,510 BP and maximum at 12,620 BP of 98 %. I_C was 44 ± 33 % with minimum of 0 % and maximum of 100 %. Eight of the twenty samples from this zone did not have any morphotypes diagnostic of C_3 and/or C_4 grass sub-families, so we were unable to calculate I_C.

Zone 2 (7750 - 2900 BP, 100 - 40 cm)

Unclassified morphotypes dominated the phytolith assemblage comprising 63 % of the total and were the largest category for every sample in zone 2. The most abundant classified morphotypes were round blocky and scalloped faceted.

RMAP was 1018 ± 121 mm for zone 2. The decline in RMAP that began in zone 3 continued, reaching a minimum of 824 mm at 6890 BP. RMAP then began a general increasing trend which continued throughout the zone with the maximum value of 1176 mm occurring at 4400 BP. RMAT was 15.9 ± 0.7 °C with minimum of 15.0 °C at 6890 BP and maximum at 3620 BP of 17.2 °C and displayed a generally increasing trend throughout zone 2.

RMAP had mean dissimilarity of 0.52 with mean sample dissimilarity minimum of 0.39 at 3250 BP and mean sample dissimilarity maximum of 0.61 at 6890 BP. RMAT mean dissimilarity was 0.60 with mean sample dissimilarity minimum of 0.42 at 3250 BP and mean sample dissimilarity maximum of 0.69 at 6890 BP. There were no dissimilarities less than 0.1580.

I_W was 78 ± 7 % with minimum of 63 % at 3250 BP and maximum of 87 % at 3620 BP. I_C was 27 ± 25 % with minimum of 0 % and maximum of 67 % at 2900 BP. Five of the thirteen samples in this zone did not have any morphotypes diagnostic of C_3 grass sub-families, so we were unable to calculate I_C.

Zone 1 (2560 - 730 BP, 35 - 0 cm)

Unclassified morphotypes were the largest category the phytolith assemblage in the zone 1 with 15 % of total phytoliths. The most abundant classified morphotypes were round blocky, other long cells, other short cells, square, and short saddles.

RMAP was 912 ± 251 mm for zone 1 with maximum of 1332 mm at 2560 BP. RMAP generally decreased reaching a minimum of 620 mm at 1640 BP followed by a gradual increase to 970 mm at 730 BP. RMAT was 14.8 ± 1.7 °C with maximum at 2560 BP of 17.1 °C declining to a minimum of 12.7 °C at 1640 BP followed by a rising trend through 730 BP

RMAP had mean dissimilarity of 0.26 with mean sample dissimilarity minimum of 0.20 at 730 BP and mean sample dissimilarity maximum of 0.31 at 1380 BP. RMAT mean dissimilarity was 0.29 with mean sample dissimilarity minimum of 0.25 at 730 BP and mean sample dissimilarity maximum at 1380 BP of 0.34. One dissimilarity value was less than 0.1580, k_1 = 0.1284 at 730 BP

I_W was 25 ± 10 % with minimum of 16 % at 730 BP and maximum of 45 % at 2560 BP. I_C was 25 ± 10 % with minimum of 13 % at 730 BP and maximum of 44 % at 2230 BP

Discussion

Reconstructed Climate

Conditions were still generally cold and dry after the Last Glacial Maximum (LGM). RMAP was less than 450 mm and RMAT under 10 °C at the beginning of our record at 17,550 BP. A prominent spike in both RMAP and RMAT occurred at 17,160 BP as RMAT rose to over 1150 mm and RMAT reached 14.6 °C. These conditions were much wetter than at present but still much cooler than today. This spike may represent the Heinrich H1 event and was followed by a return to dry and colder conditions. At 16,740 BP there was an increase in RMAP to modern values of about 800 mm accompanied by an increase in RMAT to around 13.6 °C. RMAP remained fairly stable for the next 2000 years before another sharp increase to conditions wetter than today with 1133 mm at 14,000 indicating the end of glacial conditions. RMAT also remained relatively stable but with a more gradually increasing trend. Our findings are in general agreement with those from Hall's Cave of Toomey et al. (Toomey, 1993; Toomey et al., 1993) and those of Musgrove et al. (2001) who documented the increase in stalagmite growth rates, associated with increased precipitation, in caves along the eastern edge of the Edwards Plateau during this period. They closely match the results of Ellwood and Gose (2006) who attributed a spike in magnetic susceptibility in Hall's Cave sediments at 17,160 BP to the H1 event and another at about 14,000 BP to the end of glacial conditions.

For the next 6000 years, from 14,000 BP until about 8000 BP, RMAP was generally higher than today and gradually increasing with several oscillations between modern values and about 1150 mm. The peaks in RMAP of 1133 mm at 14,000 BP and 1165 mm at 13,330 BP may have been caused by the Bølling-Allerød interstadial. By 7750 BP RMAP had fallen back to approximately modern levels. A steady increase in RMAP occurred from 6890 BP to 2560 BP when it reached the maximum level of the past 17,000 years of over 1300 mm. RMAT steadily increased reaching almost 17 °C at 11,090 BP and then stabilizing for the next 8500 years with values between 15 °C and 17 °C through 1930 BP.

Except for a peak in RMAP at 13,330 BP, our results differ from the moisture reconstructed at Hall's Cave by Toomey et al. (Toomey, 1993; Toomey et al., 1993) who found a trend of decreasing effective moisture throughout this period, although our reconstructed temperatures are in general agreement. Through 8000 BP, both our RMAP and RMAT contradict the findings of Ellwood and Gose (2006) who found a decreasing trend in magnetic susceptibility associated with cooler and dryer conditions to 10,500 BP then an increasing trend in magnetic susceptibility associated with warmer and dryer conditions with an upward spike at 8200 BP which they attributed to the 8.2 ka event. The much less prominent decrease in our RMAP and RMAT at 8170 BP may also be attributable to the 8.2 ka event but opposite in direction. After 8000 BP our findings are in general agreement with those of Ellwood

and Gose (2006). Our RMAP values from 14,000 BP through 1930 BP, which were generally higher than mean annual precipitation of today, are also in general disagreement with those of Musgrove et al. (2001) who found decreases in speleothem growth rate associated with decreased precipitation throughout this period. However, the trends in July temperature deviations reconstructed by Nordt et al. (2007) from stable carbon isotope ratios in buried soils from the central Great Plains and in global mean annual temperature deviations reconstructed by Vinther et al. (2009) from stable oxygen isotope ratios in Greenland ice cores support our results.

The Younger Dryas is apparent in the reconstructed July temperature deviations of Nordt et al. (2007) and is probably represented at the beginning of the reconstructed mean annual temperature deviations of Vinther et al. (2009). The decline in our RMAP from 13,330 BP to 11,480 BP may be associated with the Younger Dryas but RMAP only decreased to modern levels and the decline in RMAT is less obvious. Likewise, both isotope reconstructions (Nordt et al., 2007; Vinther et al., 2009) were able to discern a period of temperatures higher than those of today, the Holocene Climatic Optimum. While our highest reconstructed temperatures occurred during this same period, 7750 BP to 2560 BP, values were still lower than today and were not discernible as a significant event. Ellwood and Gose (2006) reported a less prominent feature at 4300 BP which they attributed to the 4400 BP climate shift reported by Chang and Patterson (2005). The pattern in our RMAP at the same time is very similar but also is not a prominent feature.

The maximum RMAP at 2560 BP was followed by a sharp decline with RMAP reaching 620 mm, somewhat dryer than today, at 1640 BP and was mirrored by a drop in RMAT to less than 12.7 °C. RMAP then stabilized near modern values before again becoming wetter than today with around 970 mm at 730 BP while RMAT began a warming trend reaching about 14.3 °C at 730 BP, still much cooler than today at the end of our record.

Our RMAP results are opposite to the effective moisture reconstruction of Toomey et al. (Toomey, 1993; Toomey et al., 1993) who reported that 2560 BP to 1640 BP was the latter part of the driest period in the Holocene followed by moister conditions until around 920 BP when moisture decreased to modern values. The findings of Musgrove et al. (2001) who reported very low stalagmite growth rates through the present are also inconsistent with our findings. Our results are similar to those of Elwood and Gose (2006) who reported generally increasing magnetic susceptibility peaking at 2000 BP followed by a drop that they attributed to either colder or very dry conditions. The general trends from the reconstructions of Nordt et al. (2007) and Vinther et al. (2009) during this period are consistent with our results.

Overall, our reconstructions for mean annual precipitation and mean annual temperature are in good agreement with high resolution reconstructions based on magnetic susceptibility, stable carbon isotopes, and stable oxygen isotopes. This is somewhat surprising given that only one of our

samples had even one true analog in the training data set as defined by ROC analysis and that two of the three most abundant morphotypes, round blocky and epidermal polygonal, were not used in the transfer functions. The more muted pattern in RMAT as compared to RMAP is to be expected due to the much lower statistical significance and higher dissimilarities in the reconstruction for mean annual temperature. These factors along with the general trend agreement between our RMAT and the high resolution reconstructions as well as the low magnitude of predicted temperatures when compared to other reconstructions leads us to suspect that RMAT values are underestimated. In contrast with the isotopic reconstructions, our reconstructions did not allow for the definitive discernment of either the Younger Dryas or the Holocene Climatic Optimum. Ellwood and Gose (2006) were also unable to pick out these events with much certainty. In our case, data do not seem to be a limitation in discerning these events. The mean time associated with our 5 cm sample intervals was 350 years which should be a fine enough resolution to detect signals from even short duration events such as the Younger Dryas. It is possible that the central Edwards Plateau experienced mild responses to these events, but more likely that our models are in need of additional refinement.

The disagreements between our results and those of Toomey et al. (Toomey, 1993; Toomey et al., 1993) and Musgrove et al. (2001) could be explained by a lack of detailed resolution in these reconstructions based on faunal remains and speleothem growth rates respectively. Toomey (1993) reported that changes in temperature were not great enough after 14,500 BP to be detected by faunal analysis. Musgrove et al. (2001) based their reconstructions on interpolations between dated points on speleothems with wide time ranges and very few of those dates were within the Holocene. Important changes that occurred between dated points could easily have gone undetected.

Reconstructed Vegetation

Vegetation at 17,550 BP was probably mixed grass savanna or open woodland transitioning to closed woodland and then forest by 14,940 BP. Grass abundance decreased drastically during this period to near absence, while the epidermal polygonal morphotype simultaneously increased to its maximum abundance. This forest with a near absences of grasses was representative of the vegetation through 8170 BP. The only notable change was an opening up to closed woodland at 13,670 BP. While the abundance of the epidermal polygonal morphotype dropped dramatically at 7750 BP, grass abundance remained very low as forest and woodland continued to be the norm through 2900 BP. The climatic index, I_C, was unable to provide any information for most of this period due to the paucity of grass phytoliths.

These results are quite different from those of Toomey et al. (Toomey, 1993; Toomey et al., 1993) who concluded that woodland and forest were not an important part of the Edwards Plateau

vegetation during the past 25,000 years. Fredlund (1998) reconstructed past vegetation based on phytolith assemblages from the Wilson-Leonard site on the northeastern edge of the Edwards Plateau. He recorded values of his woodland-grassland ratio indicating woodland vegetation becoming more open from 13,000 BP until 2000 BP when a trend toward more closed woodland began. These results are in general agreement with ours. Gehlbach (1991) used fossil vertebrate assemblages from locations straddling the eastern edge of the Edwards Plateau to reconstruct past vegetation with results very similar to our own. He concluded that coniferous and deciduous forest was the typical vegetation on the Edwards Plateau before 16,000 BP, when deciduous forest took over with herbs and grasses gradually expanding until around 2000 BP.

Our vegetation reconstruction showed a transition to open woodland occurring at 2560 BP accompanied by a marked increase in grass abundance. By 2230 BP more open grassland vegetation had taken hold with grass composition transitioning from mixed to C_4 dominance. At this point, forests on the Edwards Plateau had probably retreated to their present distribution along riparian zones where they remained through 730 BP. These results are in good agreement with those of Gehlback (1991) who concluded that open woodland or savanna took over the western part of the Edwards Plateau around 2000 BP. This transition differs from the shift to a more closed woodland at 2000 BP noted by Fredlund (1998).

Overall, our vegetation reconstruction is in good agreement with the findings of Gehlbach (1991). Our results are in general agreement with those of Fredlund (1998) with the exception of change to a more closed woodland he noted at 2000 BP. This could be an actual difference between vegetation at Hall's Cave and the Wilson-Leonard site at this time. However, Fredlund was uncertain of the age of that transition and he was unable to perform any more recent reconstructions due to missing soil above that point in the profile so we don't know what the trend might have been after that point. The general disagreement between our results and those of Toomey et al. (Toomey, 1993; Toomey et al., 1993) could be an issue of range. The majority of phytoliths in Hall's Cave sediments probably washed in from the 3 ha catchment area upslope from the cave, a very local area. Toomey (1993) thought the microfaunal remains in the cave were brought there by raptors and that the faunal assemblage could then originate from an area as large as the hunting range of raptors, a much larger area than the catchment area of the cave. The faunal assemblage could then be biased towards species who preferred open habitats where raptors hunt, lending itself to an interpretation of more open vegetation.

Issues and Limitations

Lack of taxonomic resolution is one of the problems inherent to reconstructions based on

phytolith assemblages. In this study unclassified morphotypes made up the majority of the distribution. Any information contained in these forms remains unavailable to us. This lack of taxonomic resolution is also an issue with classified types. Two of the three most abundant morphotypes provide an illustration of this problem. Blinnikov (2005) found the round blocky morphotype in *Abies*, *Artemisia,* and *Picea* and the epidermal polygonal morphotype in *Abies*, *Artemisia*, other Asteraceae, and several deciduous trees, as well as other shrubs and forbs. An assemblage dominated by these forms could be interpreted as a sagebrush steppe, sub-alpine forest, or a field of sunflowers.

Taxonomic resolution is better within Poaceae but this is still an issue. Barboni et al. (1999) found that their reconstruction using the Twiss (1969) classification and I_C was subject to this problem of poor taxonomic resolution. I_C relates the proportions of phytoliths from C_3 and C_4 grasses. Use of this index was complicated at their study site when they found that C_3 *Phragmites* from Arundinoideae produced the short saddle morphotype associated with the C_4 Chloridoideae. They also discovered that C_4 *Sporobolus* from Chloridoideae produced the rondels and rectangle morphotypes associated with the C_3 Pooideae. Fredlund and Tieszen (1994) suggested that analyses focused on assemblages rather than morphotypes can help alleviate this problem and showed that modern phytolith assemblages can discriminate between modern vegetation types even though most Poaceae sub-families produce most morphotypes. However, this issue can still complicate paleoreconstructions. In this study, it is quite possible that a morphotype attributed to xeric adapted C_4 vegetation assemblages today was produced by C_4 vegetation which was dominant during extremely dry periods but by C_3 vegetation that was dominant during very wet periods. Climatic predictions based on transfer functions trained on modern vegetation and phytolith assemblages could then be artificially deflated or inflated at points in the past due to morphotype production changes through time.

Another of the problems associated with phytolith based reconstructions is the lack of use of a standard classification. In this study we had to map many of the counted morphotypes onto the other or unclassified group in the classification of Lu et al. (2006) in order to use the transfer functions we developed from their training data set, including the round blocky and epidermal polygonal morphotypes. These two types were two of the most abundant types in the Hall's Cave phytolith assemblage yet they did not contribute anything to our RMAP and RMAT due to incompatible classification schemes. Lack of use of a standard classification also comes into play in model validation. Ideally we would have tested our transfer functions with modern phytolith assemblages and climatic data. However, we were unable to find any other published data set with a classification compatible with our transfer functions.

It is possible that human disturbance could have altered the phytolith assemblage. Toomey (1993) reported evidence of human presence in Hall's Cave for the past 8000 years. The most frequent evidence of human activity was the presence of hearths which we might expect to bias the

assemblage toward a higher proportion of woody morphotypes as wood was brought into the cave for fire. However, there was no increase in woody types associated with the the time of human activity. Toomey (1993) believed the hearths were probably ony used for a few days and did not find evidence of continuous occupation. It is likely that human activity was too infrequent to have a noticeable impact on the phytolith assemblage.

Conclusions

We have demonstrated the potential of paleoenvironmental reconstructions based on phytolith assemblages to improve the resolution of climate and vegetation records. However, much improvement in phytolith taxonomy and classification is needed before phytolith based reconstructions can move beyond a complementary role in quantitative paleoenvironmental reconstructions.

Our reconstruction has added to the knowledge of past precipitation, temperature, and vegetation on the Edwards Plateau from the last glacial period to the present. In particular, we were able to create a statistically significant reconstruction of past mean annual precipitation. To our knowledge this is the first phytolith based study that attempts to determine the statistical significance of a palaeoenvironmental reconstruction. We believe this is a step forward for paleoecology and agree with Telford and Birks (2011) that paleoecology should strive to hold itself to the same quantitative standards as other areas of ecology.

Disagreements between our results and those of some previous climatic and vegetation reconstructions for the Edwards Plateau, particularly the fact that our results show higher mean annual precipitation and more forested vegetation, indicate the need for additional research. Agreements with other high resolution paleoenvironmental reconstructions include clear signals probably associated with the Heinrich H1 event and the Bølling-Allerød interstadial. While still in general agreement with these reconstructions based on magnetic susceptibility and stable isotope analysis, our results were unable to clearly discern some high magnitude climatic events evident in those reconstructions such as the Younger Dryas and Holocene Climatic Optimum indicating the necessity for further model refinement.

References

Barboni, D., Bonnefille, R., Alexandre, A., Meunier, J.D., 1999. Phytoliths as paleoenvironmental indicators, West Side Middle Awash Valley, Ethiopia. Palaeogeography, Palaeoclimatology, Palaeoecology 152, 87-100.

Bennett, K.D., 1996. Determination of the number of zones in a biostratigraphical sequence. New

Phytologist 132, 155-170.

Birks, H.J.B., Berglund, B.E., 1979. Holocene pollen stratigraphy of southern Sweden: a reappraisal using numerical methods. Boreas 8, 257-279.

Blinnikov, M., Busacca, A., Whitlock, C., 2002. Reconstruction of the late Pleistocene grassland of the Columbia basin, Washington, USA, based on phytolith records in loess. Palaeogeography, Palaeoclimatology, Palaeoecology 177, 77-101.

Blinnikov, M.S., 2005. Phytoliths in plants and soils of the interior Pacific Northwest, USA. Review of Palaeobotany and Palynology 135, 71-98.

Bozarth, S.R., 1992. Classification of opal phytoliths formed in selected dicotyledons native to the Great Plains, in: Rapp, Jr., G., Mulholland, S.C. (Eds.), Phytolith Systematics: Emerging Issues, Advances in Archaeological and Museum Science. Plenum Press, New York, NY, pp. 193-214.

Brown, D.A., 1984. Prospects and limits of a phytolith key for grasses in the central United States. Journal of Archaeological Science 11, 345-368.

Chang, A.S., Patterson, R.T., 2005. Climate shift at 4400 years BP: Evidence from high-resolution diatom stratigraphy, Effingham Inlet, British Columbia, Canada. Palaeogeography, Palaeoclimatology, Palaeoecology 226, 72-92.

Cooke, M.J., Stern, L.A., Banner, J.L., Mack, L.E., Stafford, T.W., Toomey, R.S., 2003. Precise timing and rate of massive late Quaternary soil denudation. Geology 31, 853 -856.

Cordova, C.E., Johnson, W.C., Mandel, R.D., Palmer, M.W., 2011. Late Quaternary environmental change inferred from phytoliths and other soil-related proxies: case studies from the central and southern Great Plains, USA. CATENA 85, 87-108.

Ellwood, B.B., Gose, W.A., 2006. Heinrich H1 and 8200 yr B.P. climate events recorded in Hall's Cave, Texas. Geology 34, 753-756.

Fredlund, G., 1998. Phytolith analysis, in: Collins, M.B., Bousman, C.B., Bailey, G.L.. (Eds.), Wilson-Leonard: An 11,000-year Archeological Record of Hunter-gatherers in Central Texas, Studies in Archaeology. Texas Archeological Research Laboratory, University of Texas at Austin, Austin Texas, pp. 1637-1656.

Fredlund, G.G., Tieszen, L.L., 1997. Calibrating grass phytolith assemblages in climatic terms: application to late Pleistocene assemblages from Kansas and Nebraska. Palaeogeography, Palaeoclimatology, Palaeoecology 136, 199-211.

Fredlund, G.G., Tieszen, L.T., 1994. Modern phytolith assemblages from the North American Great Plains. Journal of Biogeography 21, 321-335.

Gehlbach, F.R., 1991. The east-west transition zone of terrestrial vertebrates in central Texas - a biogeographical analysis. Texas Journal of Science 43, 415-427.

Griffith, G.E., Bryce, S.A., Omnerik, J.M., Rogers, A.C., 2007. Ecoregions of Texas (Project report). Texas

Commission of Environmental Quality.

Grimm, E.C., 1987. CONISS: a FORTRAN 77 program for stratigraphically constrained cluster analysis by the method of incremental sum of squares. Computers & Geosciences 13, 13-35.

Hill, M.O., 1973. Diversity and evenness: a unifying notation and its consequences. Ecology 54, 427.

Juggins, S., 2011. Rioja: analysis of quaternary science data.

Klein, R.L., Geis, J.W., 1978. Biogenic silica in the Pinaceae. Soil Science 126, 145–156.

Kondo, R., Childs, C., Atkinson, I., 1994. Opal phytoliths of New Zealand. Manaaki Whenua Press, Lincoln, New Zealand.

Lentfer, C.J., Boyd, W.E., 1998. A comparison of three methods for the extraction of phytoliths from sediments. Journal of Archaeological Science 25, 1159-1183.

Lu, H., Liu, K.-biu, 2003. Phytoliths of common grasses in the coastal environments of southeastern USA. Estuarine, Coastal and Shelf Science 58, 587-600.

Lu, H.-Y., Wu, N.-Q., Liu, K.-B., Jiang, H., Liu, T.-S., 2007. Phytoliths as quantitative indicators for the reconstruction of past environmental conditions in China II: palaeoenvironmental reconstruction in the Loess Plateau. Quaternary Science Reviews 26, 759-772.

Lu, H.-Y., Wu, N.-Q., Yang, X.-D., Jiang, H., Liu, K.-biu, Liu, T.-S., 2006. Phytoliths as quantitative indicators for the reconstruction of past environmental conditions in China I: phytolith-based transfer functions. Quaternary Science Reviews 25, 945-959.

Madella, M., Alexandre, A., Ball, T., 2005. International Code for Phytolith Nomenclature 1.0. Annals of Botany 96, 253 -260.

Musgrove, M., Banner, J.L., Mack, L.E., Combs, D.M., James, E.W., Cheng, H., Edwards, R.L., 2001. Geochronology of late Pleistocene to Holocene speleothemsfrom central Texas: Implications for regional paleoclimate. Geological Society of America Bulletin 113, 1532-1543.

National Climatic Data Center, 2011. NCDC web climate services version 2.5 (WWW Document). NCDC Web Climate Services version 2.5. URL http://www.ncdc.noaa.gov/oa/climate/stationlocator.html

Nordt, L., von Fischer, J., Tieszen, L., 2007. Late Quaternary temperature record from buried soils of the North American Great Plains. Geology 35, 159-162.

Ollendorf, A.L., 1992. Toward a chassification scheme of sedge (Cyperaceae) phytoliths., in: Rapp, Jr., G., Mulholland, S.C. (Eds.), Phytolith Systematics: Emerging Issues, Advances in Archaeological and Museum Science. Plenum Press, New York, NY, pp. 91-106.

Overpeck, J.T., Webb, T., Prentice, I.C., 1985. Quantitative interpretation of fossil pollen spectra: dissimilarity coefficients and the method of modern analogs. Quaternary Research 23, 87-108.

Pearsall, D.M., Dinan, E.H., 1992. Developing a phytolith classification system, in: Rapp, Jr., G., Mulholland, S.C. (Eds.), Phytolith Systematics: Emerging Issues, Advances in Archaeological and

Museum Science. Plenum Press, New York, NY, pp. 37-64.

Piperno, D.R., 2006. Phytoliths: A Comprehensive Guide for Archaeologists and Paleoecologists. AltaMira Press.

Piperno, D.R., Pearsall, D.M., 1998. The silica bodies of tropical American grasses: morphology, taxonomy, and implications for grass systematics and fossil phytolith identification, Smithsonian contributions to botany. Smithsonian Institution Press, Washington, D.C.

Prebble, M., Schallenberg, M., Carter, J., Shulmeister, J., 2002. An analysis of phytolith assemblages for the quantitative reconstruction of late Quaternary environments of the Lower Taieri Plain,Otago, South Island, New Zealand I. Modern assemblages and transfer functions. Journal of Paleolimnology 27, 393-413.

Prebble, M., Shulmeister, J., 2002. An analysis of phytolith assemblages for the quantitative reconstruction of late Quaternary environments of the Lower Taieri Plain, Otago, South Island, New Zealand II. Paleoenvironmental reconstruction. Journal of Paleolimnology 27, 415-427.

Riskind, D.H., Diamond, D.D., 1988. An introduction to environments and vegetation., in: Amos, B.B., Gehlbach, F.R. (Eds.), Edwards Plateau Vegetation, Plant Ecological Studies in Central Texas. Baylor University Press, Waco, Texas, pp. 1-16.

Runge, F., 1999. The opal phytolith inventory of soils in central Africa —quantities, shapes, classification, and spectra. Review of Palaeobotany and Palynology 107, 23-53.

Simpson, G.L., Oksanen, J., 2011. analogue: analogue matching and modern analogue technique transfer function models.

Team, R.D.C., 2011. R: a language and environment for statistical computing. Vienna, Austria.

Telford, R.J., 2011. palaeoSig: significance tests of quantitative palaeoenvironmental reconstructions.

Telford, R.J., Birks, H.J.B., 2011. A novel method for assessing the statistical significance of quantitative reconstructions inferred from biotic assemblages. Quaternary Science Reviews 30, 1272-1278.

ter Braak, C.J.F., Juggins, S., 1993. Weighted averaging partial least squares regression (WA-PLS): an improved method for reconstructing environmental variables from species assemblages. Hydrobiologia 269-270, 485-502.

Toomey, R.S., 1993. Late Pleistocene and Holocene faunal and environmental changes at Hall's Cave, Kerr County, Texas (Ph.D. Dissertation).

Toomey, R.S., Blum, M.D., Valastro, S., 1993. Late Quaternary climates and environments of the Edwards Plateau, Texas. Global and Planetary Change 7, 299-320.

Toomey, R.S., Huebner, J.A., Boutton, T.W., 1992. Stable carbon isotope ratios of Equus sp. and Bison antiquus from the Late Pleistocene deposits at Hall's Cave, Kerr County, Texas. Current Research in the Pleistocene 9, 112–114.

Twiss, P.C., 1987. Grass-opal phytoliths as climatic indicators of the Great Plains Pleistocene, in: Johnson,

W.C. (Ed.), Quaternary Environments of Kansas, Kansas Geological Survey Guidebook Series. Kansas Geological Survey, University of Kansas, pp. 179-188.

Twiss, P.C., Suess, E., Smith, R.M., 1969. Morphological classification of grass phytoliths. Soil Science Society of America Journal 33, 109–115.

Vinther, B.M., Buchardt, S.L., Clausen, H.B., Dahl-Jensen, D., Johnsen, S.J., Fisher, D.A., Koerner, R.M., Raynaud, D., Lipenkov, V., Andersen, K.K., Blunier, T., Rasmussen, S.O., Steffensen, J.P., Svensson, A.M., 2009. Holocene thinning of the Greenland ice sheet. Nature 461, 385-388.

Wahl, E.R., 2004. A general framework for determining cutoff values to select pollen analogs with dissimilarity metrics in the modern analog technique. Review of Palaeobotany and Palynology 128, 263-280.

Zhao, Z., Pearsall, D.M., 1998. Experiments for improving phytolith extraction from soils. Journal of Archaeological Science 25, 587-598.

Table 1: Sample depths, ages, and associated lithology. Ages are in calibrated ^{14}C years after Ellwood and Gose (2006). Lithology is from Toomey (1993) and Ellwood and Gose (2006).

Depth (cm)	Age (BP)	Lithology
0	730	
5	920	
10	1140	
15	1380	black clayey silt
20	1640	
25	1930	
30	2230	
35	2560	
40	2900	
45	3250	
50	3620	
55	4000	
60	4400	
65	4800	
70	5200	dark brown clayey silt
75	5620	
80	6040	
85	6460	
90	6890	
95	7320	
100	7750	
105	8170	
110	8600	
115	9030	
120	9450	
125	9860	red-brown clayey silt
130	10280	
135	10690	
140	11090	
145	11480	
150	11870	
155	12250	
160	12620	
165	12980	
170	13330	red-tan silty clay
175	13670	
180	14000	
185	14330	
190	14640	
195	14940	
205	15510	
215	16040	
230	16740	
235	16960	yellow-brown sandy clay
240	17160	

Depth (cm)	Age (BP)	Lithology
245	17360	
250	17550	

Table 2: Phytolith morphotypes as counted with references, their mapping onto the classification of Lu et al. (2006), use and classification in the calculation of I_w, and use and classification in calculation of I_c.

Counted	References	Lu et al. (2006)	I_W	I_C
Keeled	Fredlund and Tieszen (1994, 1997)	Rondel	grass	C_3
Conical	Fredlund and Tieszen (1994, 1997)	Rondel	grass	C_3
Pyramidal	Fredlund and Tieszen (1994, 1997)	Rondel	grass	C_3
Round and trapezoidal	Twiss et al. (1969), Brown (1984), Cordova et al. (2011)	Rondel	grass	C_3
Long wavy trapezoidal	Fredlund and Tieszen (1994, 1997)	Wavy-trapezoid	grass	C_3
Stipa-type	Fredlund and Tieszen (1994, 1997)	Other	grass	C_3
Long straight trapezoidal	Twiss et al. (1969), Brown (1984), Cordova et al. (2011)	Wavy-narrow-trapezoid	grass	C_3
Panicoid bilobates	Fredlund and Tieszen (1994, 1997), Lu and Liu (2003), Piperno (2006)	Panicoid (dumbbell and cross)	grass	C_4
Polylobates	Twiss et al. (1969), Piperno (2006)	Other	grass	C_4
Crosses	Piperno (2006), Cordova et al. (2011)	Panicoid (dumbbell and cross)	grass	C_4
Two-side horned panicoid	Piperno (2006)	Other	grass	C_4
Short saddles	Fredlund and Tieszen (1994, 1997), Piperno (2006)	Short saddle	grass	C_4
Ellipsoid saddles(Spartina-type)	Lu and Liu (2003)	Other	grass	C_4
Aristida-type bilobates	Piperno (2006)	Other	grass	C_4
Plateau saddles (Phragmites-type)	Piperno and Pearsall (1998)	Other	grass	
Long saddles	Kondo et al. (1994), Piperno (2006)	Long saddle	grass	
Bamb and oryz types	Piperno (2006)	Other	grass	C_3
Other bilobates		Other	grass	
Flat towers	Lu and Liu (2003)	Other	grass	
Horned towers and spools	Lu and Liu (2003)	Other	grass	
Other short cells		Other	grass	
Smooth	Twiss et al. (1969), Kondo et al. (1994), Lu et al. (2006)	Smooth-elongate	grass	
Sinuous	Twiss et al. (1969), Kondo et al. (1994), Lu et al. (2006)	Sinuate-elongate	grass	
Serrated	Pearsall and Dinan (1992)	Sinuate-elongate	grass	
Echinate	Twiss et al. (1969), Madella et al. (2005)	Sinuate-elongate	grass	
Dendritic	Blinnikov et al. (2002)	Sinuate-elongate	grass	
Long point	Kondo et al. (1994), Lu et al. (2006)	Long-point	grass	
Short pointy	Kondo et al. (1994), Lu et al. (2006)	Short-point	grass	
Fan-bamboo	Lu et al. (2006)	Fan-bamb	grass	
Fan-reed	Lu et al. (2006)	Fan-reed	grass	
Fan	Lu et al. (2006)	Fan	grass	
Square	Kondo et al. (1994), Lu et al. (2006)	Square	grass	
Rectangular	Kondo et al. (1994), Lu et al. (2006)	Rectangle	grass	
Board elongate	Lu et al. (2006)	Board-elongate	grass	
Other long cells		Other	grass	
Cyperaceae-type papillae	Ollendorf (1992), Madella et al. (2005)	Other		
Asteraceae platelets	Bozarth (1992)	Other		
Celtis type	Bozarth (1992), Fredlund (1998)	Broad-leaf-type	woody	
Round blocky	Blinnikov et al. (2002; 2005)	Other	woody	
Scalloped faceted	Runge (1999)	Broad-leaf-type	woody	
Conifer type	Klein and Geis (1978), Bozarth (1992), Blinnikov (2005)	Gymnosperm types	woody	

Counted	References	Lu et al. (2006)	I_W	I_C
Round stellate	Runge (1999)	Palmaceae phytolith		
Pteridophytes	Lu et al. (2006)	Pteridophyte types		
Platanus type	Bozarth (1992)	Broad-leaf-type	woody	
Gobbet - irregular	Lu et al. (2006)	Gobbett (nubby-irregular)		
Epidermal polygonal	Blinnikov (2005)	Other		
Maclura type	Cordova et al. (2011)	Broad-leaf-type	woody	
Globular	Madella (2005)	Other		
Globular stellate	Madella (2005)	Other		
Unclassified		Other		

Figure 1: Location of Hall's Cave and the Edwards Plateau.

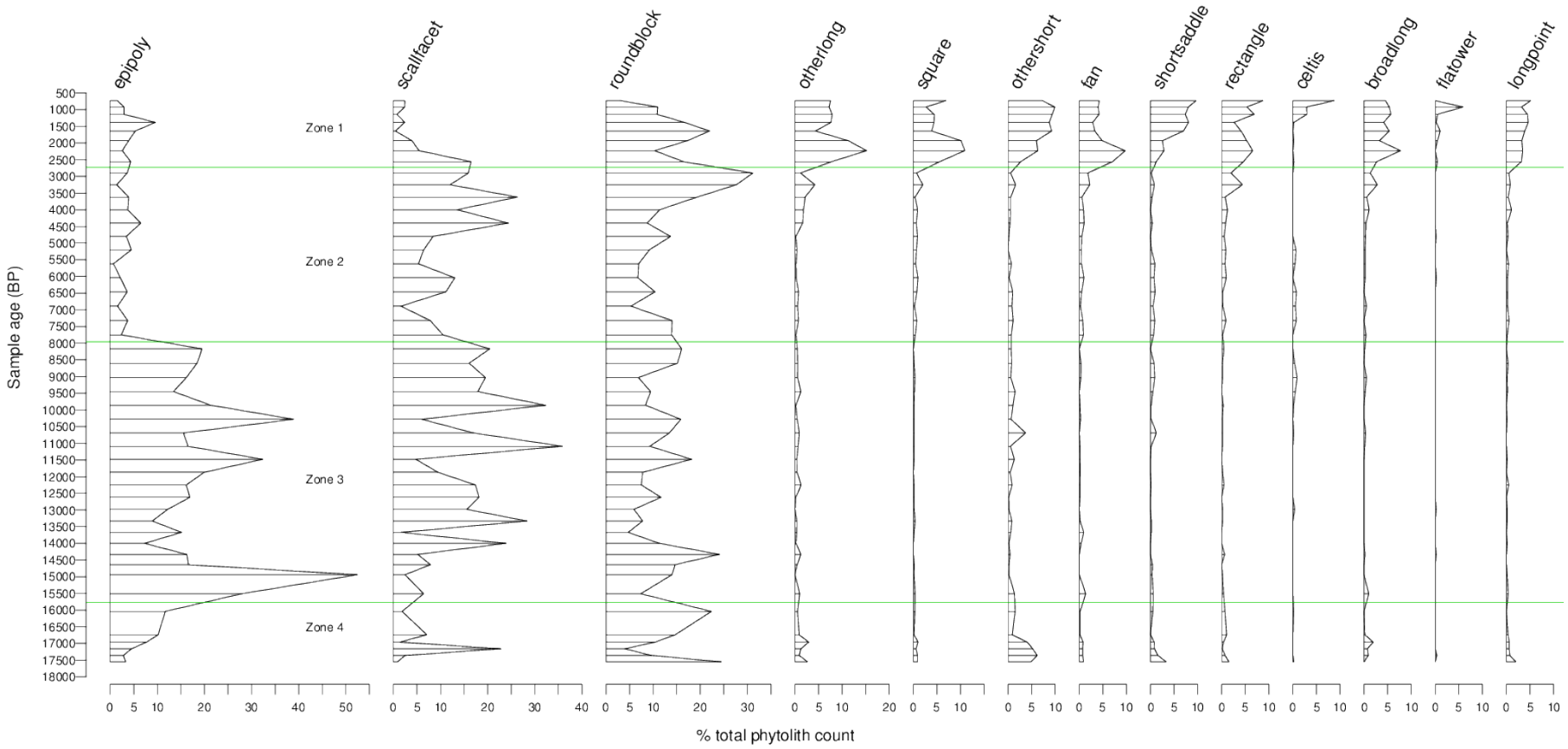

Figure 2: Phytolith morphotypes counted with at least five percent abundance in at least one sample. Morphotype abbreviations are: epipoly = Epidermal polygonal, scallfacet = Scalloped faceted, roundblock = Round blocky, otherlong = Other long cells, square = Square, othershort = Other short cells, fan = Fan, shortsaddle = Short saddles, rectangle = Rectangular, celtis = Celtis type, broadlong = Board elongate, flatower = Flat towers, longpoint = Long point.

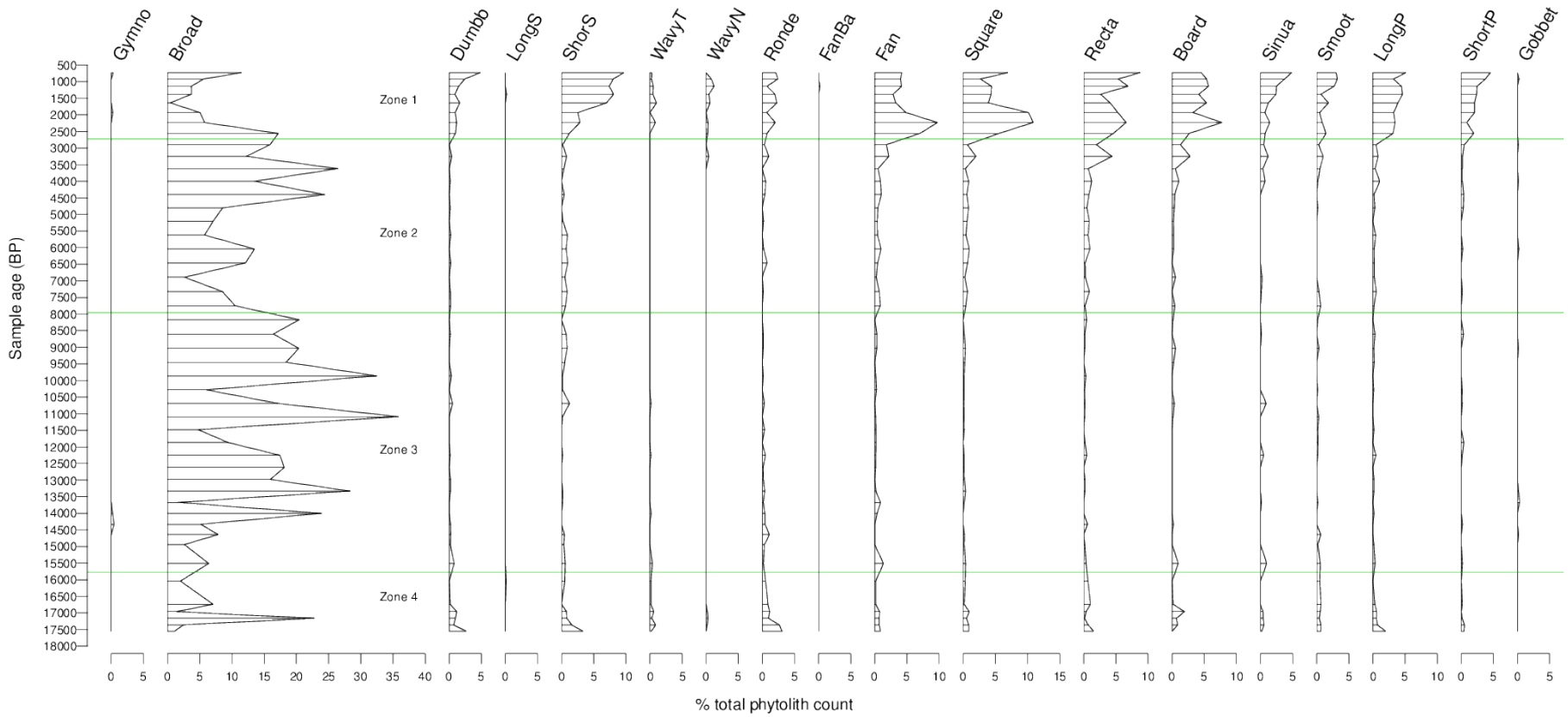

Figure 3: Phytolith morphotypes used in transfer functions with non-zero percentage in at least one sample. Morphotype abbreviations are: Gymno = Gymnosperm types, Broad = Broad-leaf-type, Dumbb = Panicoid (Dumbbell and cross), LongS = Long saddle, ShortS = Short saddle, WavyT = Wavy-trapezoid, WavyN = Wavy-narrow-trapezoid, Ronde = Rondel, FanBa = Fan-bamb, Fan = Fan, Square = Square, Recta = Rectangle, Board = Board-elongate, Sinua = Sinuate-elongate, Smoot = Smooth-elongate, LongP = Long-point, ShortP = Short point, Gobbet = Gobbett (nubby-irregular shape).

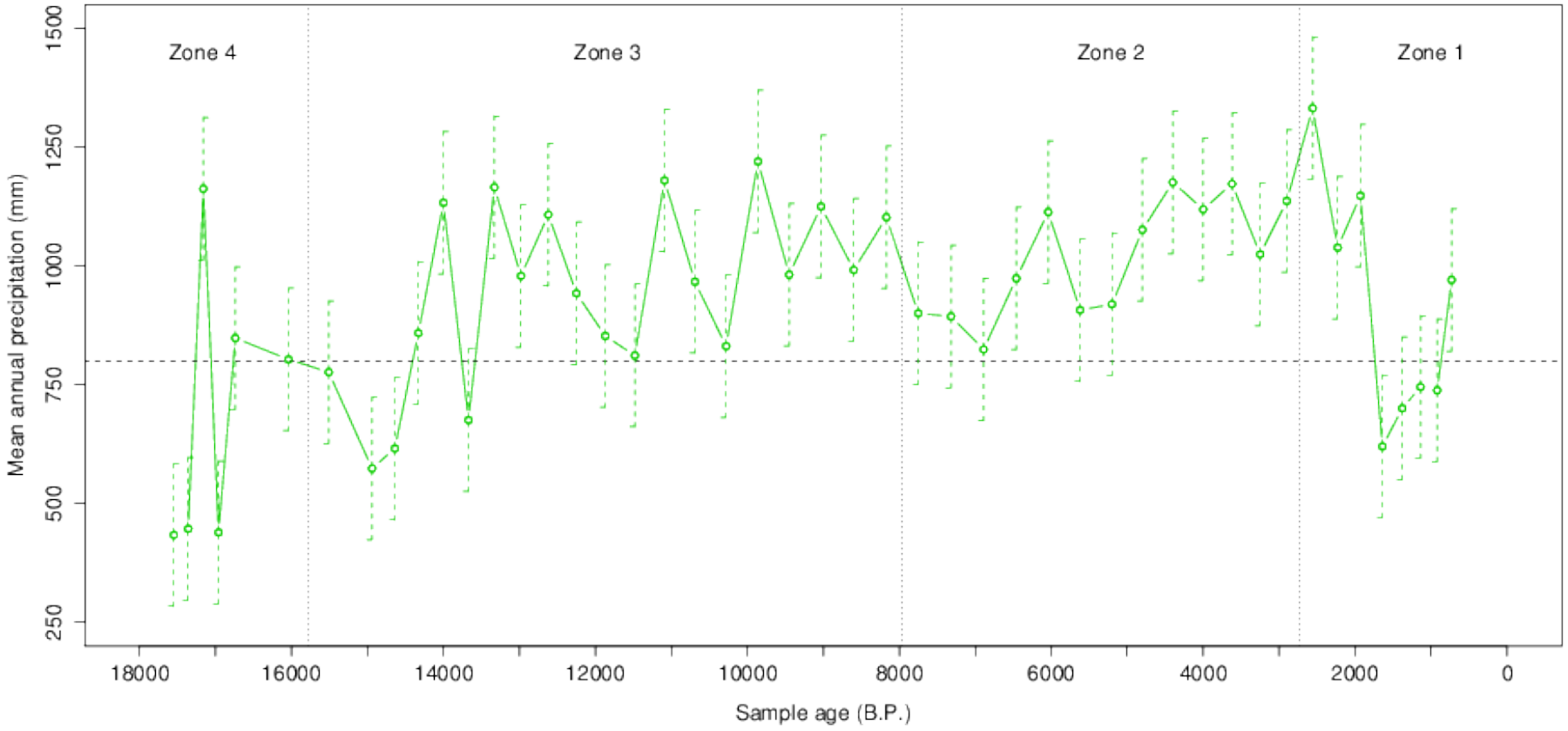

Figure 4: MAT reconstructed mean annual precipitation. Vertical dotted lines represent zone boundaries. Horizontal dashed line shows modern value of mean annual precipitation. Error bars indicate $RMSEP_{loo}$.

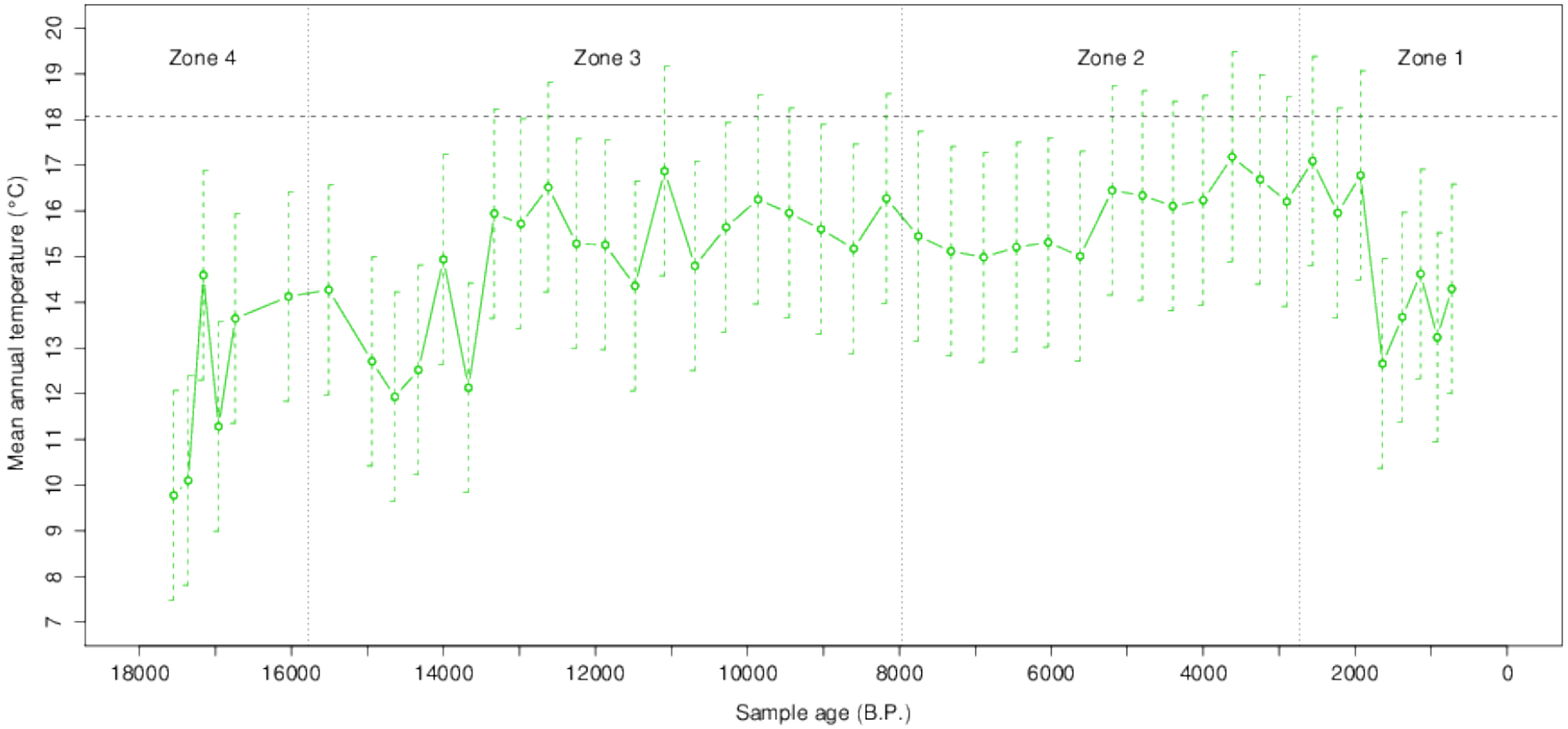

Figure 5: MAT reconstructed mean annual temperature. Vertical dotted lines represent zone boundaries. Horizontal dashed line shows modern value of mean annual temperature. Error bars indicate $RMSEP_{loo}$.

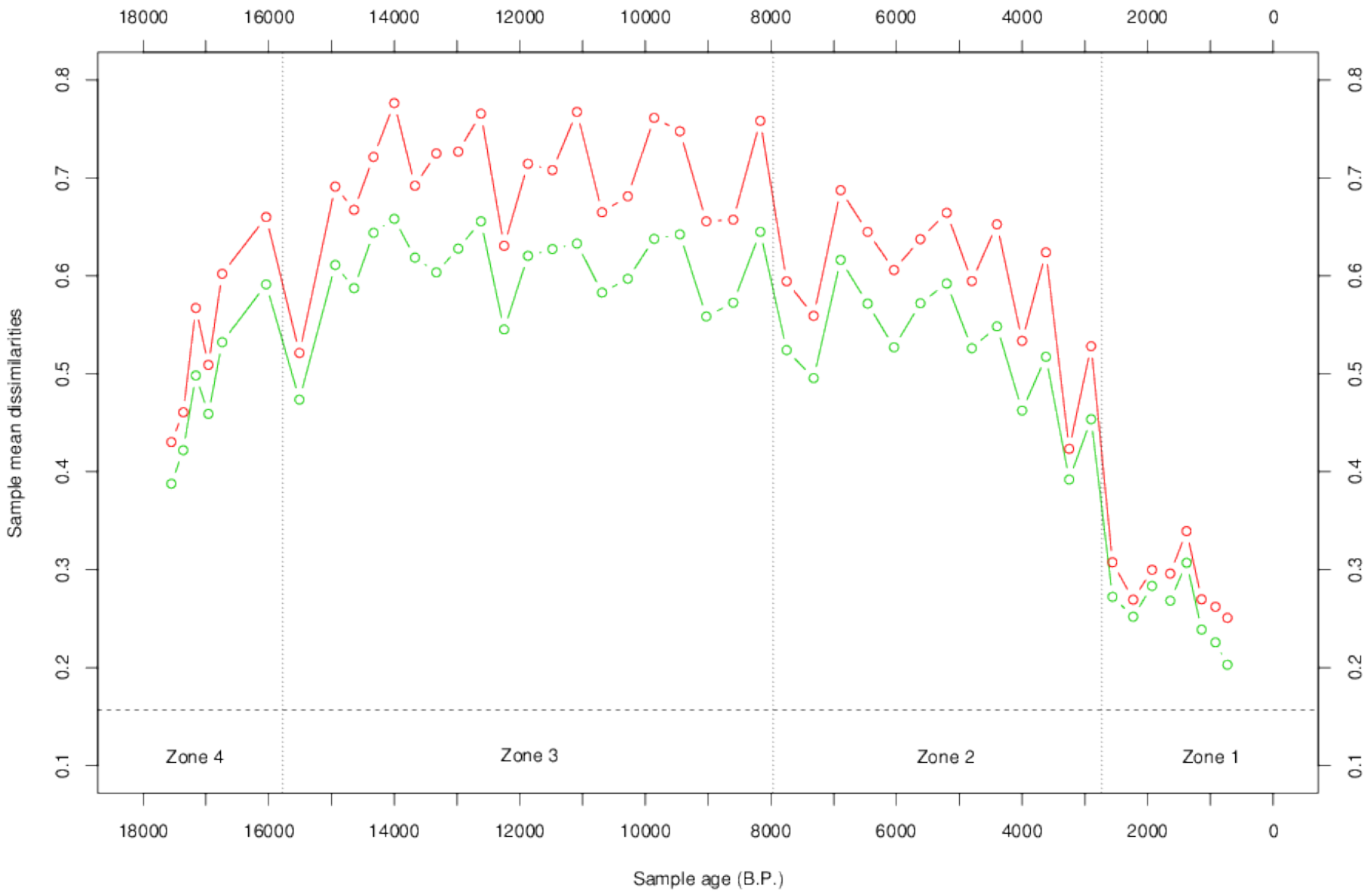

Figure 6: Dissimilarity values (squared chord distance) for mean annual precipitation (green, k = 6) and mean annual temperature (red, k = 14). Horizontal dashed line represents optimal dissimilarity value determined by ROC analysis. Vertical dotted lines represent zone boundaries. Minimum possible dissimilarity is 0 and maximum is 2.

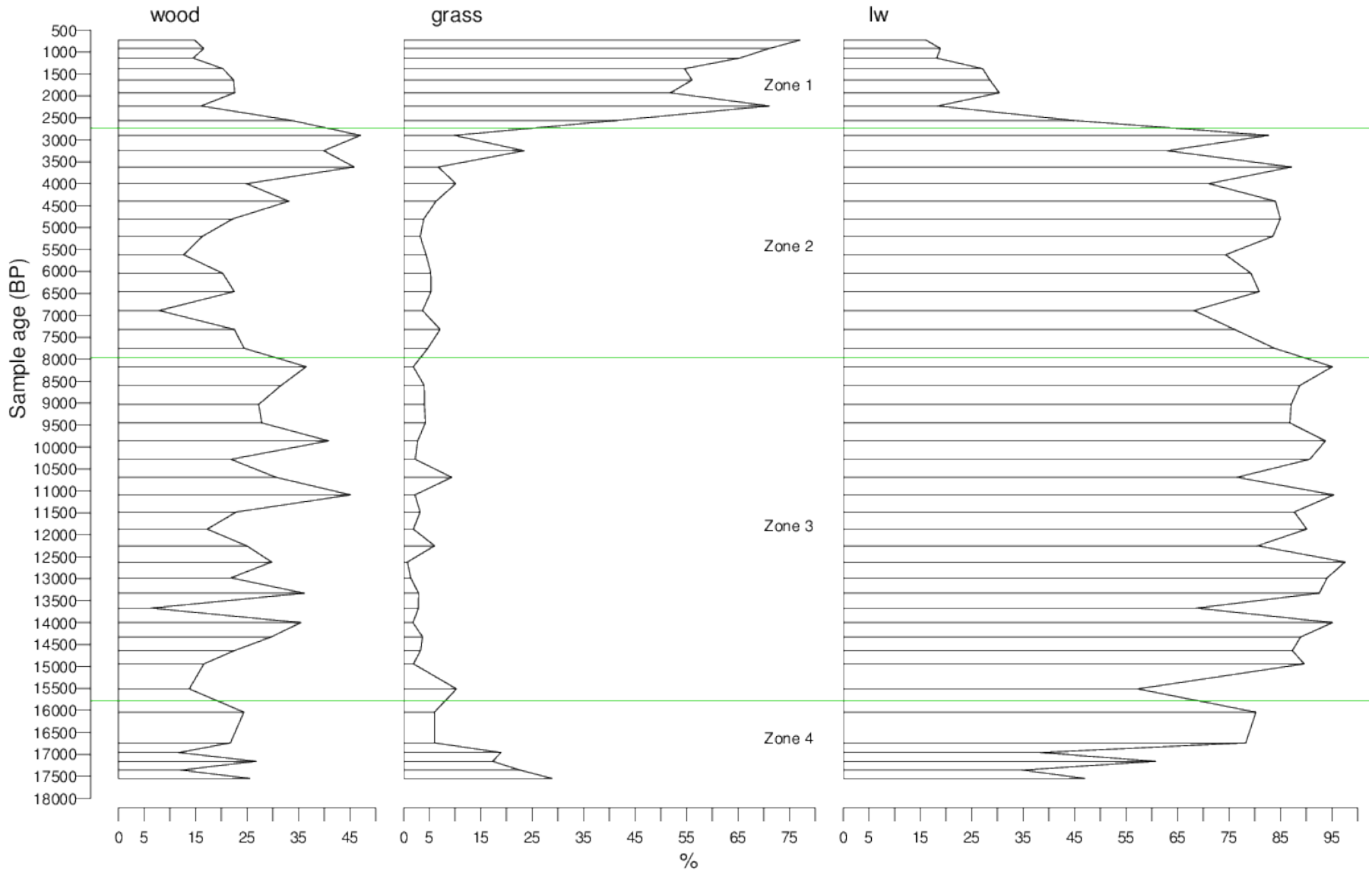

Figure 7: Phytoliths from grasses and woodies used in the calculation of I_w as percentage of total phytoliths along with I_w.

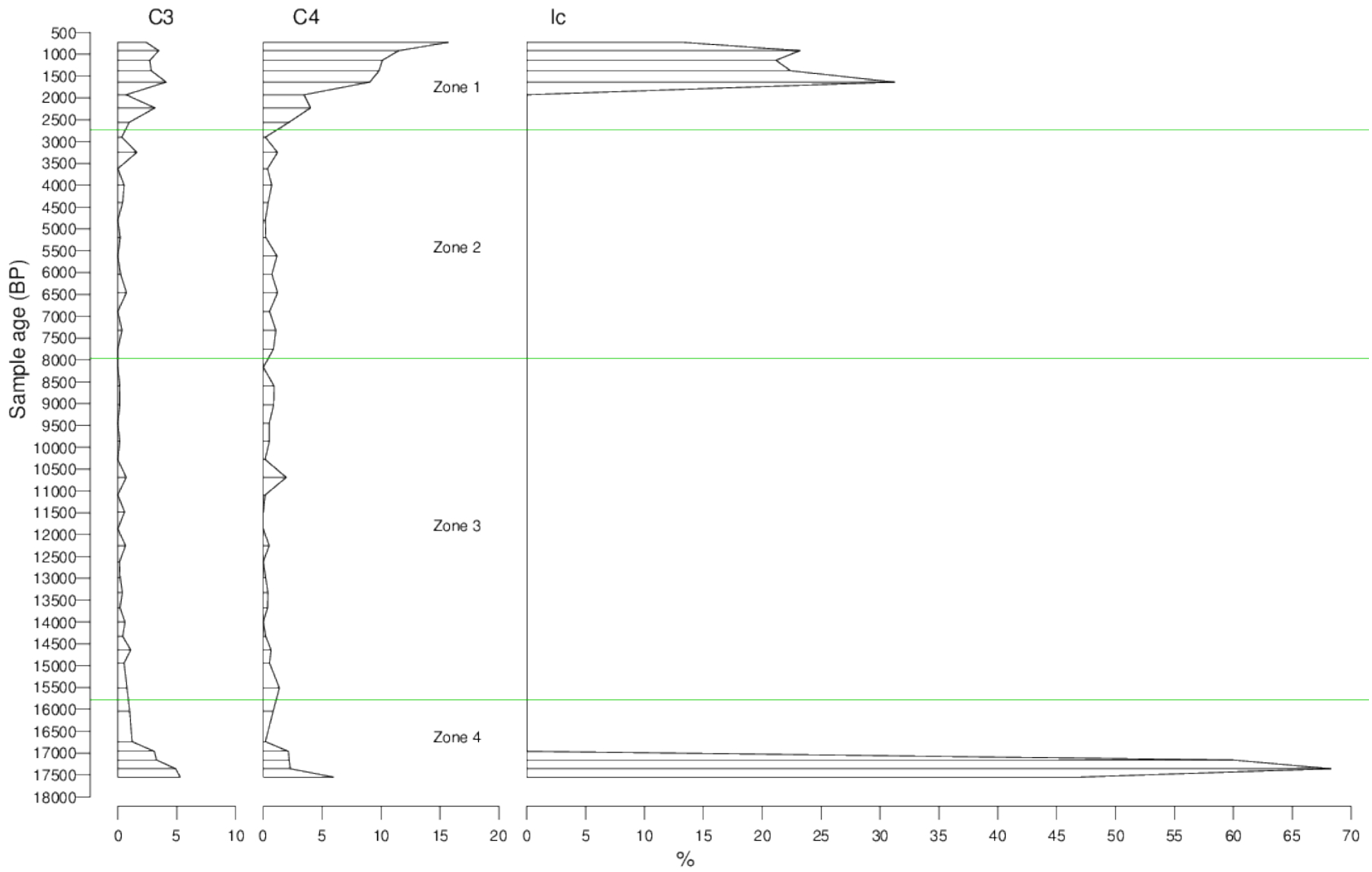

Figure 8: Phytoliths attributed to grass sub-families dominated by the C_3 or C_4 or photosynthetic pathway and used in the calculation of I_c along with I_c. I_c shown only for samples where total phytoliths used in calculation totaled at least 30.

Appendix. Supplemental electronic data

Morphotype abundances for the phytolith assemblage data are available in the file hallscaveassemblage.csv available with the online version of this document. Morphotypes are abbreviated. They are listed in the same order, and correspond to the names in the Count column of Table 2.

VITA

Jason Paul Joines

Candidate for the Degree of

Master of Science

Thesis: 17,000 YEARS OF CLIMATE CHANGE: THE PHYTOLITH RECORD FROM HALL'S CAVE, TEXAS

Major Field: Natural and Applied Sciences

Biographical:

Education: Received Bachelor of Science Degree in Geography from Oklahoma State University in May, 2005; completed the requirements for the Master of Science Degree in Natural and Applied Sciences, Natural Sciences option, from Oklahoma State University in December, 2011.

Professional memberships: Ecological Society of America, Society for Phytolith Research.

Name: Jason Paul Joines Date of Degree: December, 2011

Institution: Oklahoma State University Location: Stillwater, Oklahoma

Title of Study: 17,000 YEARS OF CLIMATE CHANGE: THE PHYTOLITH RECORD FROM HALL'S CAVE, TEXAS

Pages in Study: 35 Candidate for the Degree of Master of Science

Major Field: Natural and Applied Sciences

Scope and Method of Study: We used modern analog technique to develop phytolith-based transfer functions. We applied these transfer functions to phytolith assemblages in sediments from Hall's Cave, Texas to reconstruct mean annual precipitation and temperature for the central Edwards Plateau from 17,550 BP to 730 BP and tested these reconstructions for statistical significance. We also interpreted the phytolith assemblage and applied phytolith indices of woody cover and of C_3 versus C_4 grasses to reconstruct Edwards Plateau vegetation over the same period.

Findings and Conclusions: Reconstructed mean annual precipitation (RMAP) was less than 450 mm during the last glacial period with the exception of a spike to over 1150 mm at 17,160 BP. As glacial conditions ended RMAP progressively increased with oscillations between modern (800 mm) and higher values until reaching a high of over 1200 mm at 9860 BP. Then RMAP gradually decreased to less than 825 mm at 6890 BP followed by a gradual increase to over 1325 mm at 2560 BP. RMAP then dropped sharply to less than 625 mm at 1640 BP followed by an increase to above modern values by 730 BP. Reconstructed mean annual temperature (RMAT) followed a similar trend. RMAT was much cooler than present with a minimum of less than 10 °C during the last glacial period. RMAT also spiked at 17,160 BP approaching 15 °C before declining again. After glacial conditions ended RMAT generally increased reaching 17 °C by 3620 BP. After 2560 BP RMAT declined sharply to near 12.5 °C at 1640 BP before increasing again reaching 14 °C by 730 BP. RMAP proved to be statistically significant. We also have confidence in the trend exhibited by RMAT but temperatures may be underestimated.

Vegetation on the Edwards Plateau near the end of the last glacial period was open woodland or savanna with mixed C_3 and C_4 grasses changing to closed woodland by 16,740 BP and transitioning to forest by 14,940 BP with grasses nearly absent. Forest with little or no grass was the most common vegetation for the next 12,000 years. Open woodland or savanna with mixed C_3 and C_4 grasses re-appeared at 2560 BP transitioning to a mixed C_3 and C_3 grassland by 2230 BP and to C_4 grassland by 730 BP.

ADVISER'S APPROVAL: Carlos E. Cordova